# Magnetic anisotropy and spin coupling in a Cobalt(II) dimer with bioinspired bridges

A. F. S. Almeida,[1] A. C. das Neves,[2] Paula Brandão,[3] Mariem Masmoudi,[3] Luis Ghivelder,[4] Clebson Cruz,[5] and Mario Reis[6,*]

[1] *Instituto de Física Armando Dias Tavares, Universidade do Estado do Rio de Janeiro, R. São Francisco Xavier 524, 20550-900*[†]
[2] *Centro de Ciências Naturais e Humanas, Universidade Federal do ABC, Santo André, 09210-580*
[3] *Department of Chemistry, CICECO, University of Aveiro, Aveiro, 3810-193*
[4] *Instituto de Física, Universidade Federal do Rio de Janeiro, Av. Athos da Silveira Ramos 149, 21941-909*
[5] *Centro das Ciências Exatas e das Tecnologias, Universidade Federal do Oeste da Bahia, Rua Bertioga 892, Morada Nobre, 47810-059*
[6] *Instituto de Física, Universidade Federal Fluminense, Av. Gal. Milton Tavares de Souza s/n, 24210-346, Niteroi-RJ, Brazil*

(Dated: January 29, 2026)

**Abstract:** Cobalt(II) metal complexes constitute a versatile platform for investigating how coordination geometry and spin–orbit coupling determine its magnetic properties. Although numerous cobalt(II) coordination complexes have been reported in recent literature, only a limited number exhibit a comprehensive and quantitatively reliable magnetic characterization. In this work, we investigate the magnetic properties of the the hexacoordinated cobalt dimer $[Co_2(\mu\text{-L1H})_2(\mu\text{-}H_2O)_2(H_2O)_4]4NO_3 \cdot 2H_2O$, where L1H denotes the adenine bridging ligand . The hexacoordinated environment stabilizes a high-spin $S = 3/2$ configuration for both Co(II) centers, resulting in strong spin–orbit coupling and significant zero-field splitting, descri axial ($D$) and rhombic ($E$) anisotropy parameters. Fits to magnetic susceptibility and magnetization data reveal antiferromagnetic coupling between the Co(II) ions, with ratio $E/D \approx 1/4$ and $D/k_B = 89$ K, evidencing pronounced magnetic anisotropy in the system. This behavior is further supported by anisotropic Landé factors, $g_x = g_y = 2.5$ and $g_z = 2.4$, consistent with an easy-plane magnetic anisotropy.

**Keywords:** Hexacoordinated Co(II), Molecular magnetism, Zero-field splitting, magnetic anisotropy, adenine bridging

## I. INTRODUCTION

The study of metal complexes lay the groundwork for a broad spectrum of technologies, from magnetic refrigeration [1], high-density magnetic recording [2], and spintronics [3] to catalysis [4, 5] and biomedical applications [6]. Certain metal–organic compounds also exhibit noteworthy cytotoxic activity [7–10] and have begun to feature in emerging quantum devices such as quantum batteries and quantum thermodynamic devices [11, 12]. Within this broad landscape of metal–organic systems, dinuclear transition-metal complexes occupy a particularly relevant position, as they provide well-defined magnetic units in which exchange interactions and anisotropy effects can be quantitatively assessed [1, 13, 14]. In this context, adenine-based coordination compounds offer structurally robust frameworks capable of stabilizing closely spaced metal centers, making them suitable model systems for detailed magnetochemical investigations [6, 15].

At the same time, although numerous Co(II) complexes have been reported, only a limited number of these exhibited a complete and consistent determination of magnetic anisotropy parameters, as supported by both magnetometry and spectroscopy data. This limited availability of well-characterized systems hampers a deeper understanding of how spin–orbit coupling rules the magnetic behavior of such systems.

From this perspective, the present work examines the dinuclear cobalt complex, the dinuclear cobalt complex $[Co_2(\mu\text{-L1H})_2(\mu\text{-}H_2O)_2(H_2O)_4]4NO_3 \cdot 2H_2O$ (compound I), where L1H = adenine. The dinuclear cobalt complex investigated here was originally synthesized and structurally characterized by Masmoudi et al. [15] in the context of cytotoxic studies involving adenine-based coordination compounds. While that work focused primarily on the biological activity of the system, the magnetic properties of this compound remained unexplored. In the present study, we shift the emphasis to a detailed magnetic characterization of compound I, aiming to elucidate its anisotropy and magnetic coupling mechanisms. Such an analysis contributes to the growing body of studies on molecular magnetic systems, for which precise and quantitative magnetic parameters are essential to assess their physical behavior and potential relevance in broader condensed-matter and quantum-magnetism contexts [11, 12, 16, 17].

In this regard, by providing a comprehensive experimental–theoretical characterization of compound I, our work offers valuable reference data for ongoing efforts to correlate structure, anisotropy, and function in Co-metal complexes. Following a description of its crystal structure, we propose an effective magnetic Hamilto-

* marioreis@id.uff.br
† almeida.alan@posgraduacao.uerj.br

nian, present magnetization and $\chi T$ measurements, and analyse the model against both data. The extracted parameters give quantitative information on exchange interactions, anisotropy, and the mechanisms that govern the magnetic response of the complex, and the comprehensive magnetic characterization reported provides consistent parameters for comparison of future studies on anisotropy-driven phenomena in cobalt(II) molecular systems, highlighting the role of anisotropy in hexacoordinated compounds.

## II. EXPERIMENTAL

### A. Synthesis

The dinuclear Cobalt(II) was synthesized by the reaction, in 15 mL of ethanol, of cobalt nitrate hexahydrate (1.0 mmol, 0.291 g), and adenine (1.0 mmol, 0.135 g) under continuous stirring conditions at room temperature for 2 hours. Pink plate-like crystals suitable for single X-ray analysis were obtained by slow evaporation of the resultant solution. Elemental analysis (%): Calc. (based on single-crystal data) for $C_{10}H_{26}N_{14}O_{20}Co_2$,: C, 15.4; H, 3.3; N, 25.1; Found: C, 15.9; H, 3.5; N, 25.5.

The IR spectrum show the characteristic bands of adenine. The n($NH_2$) appears at 3115 $cm^{-1}$ and the n($NH_2$) is found at 1510 $cm^{-1}$. The n(C=C) and n(C=N) vibrations of the heterocyclic ring are observed as a broad band at 1566 $cm^{-1}$ and 1677 $cm^{-1}$ respectively. With respect to the vibrations of the nitrate group, the typical band appears at 1387 $cm^{-1}$. The weak peaks at 544 $cm^{-1}$ and 551 $cm^{-1}$ could be associated with metal-nitrogen and metal-oxygen vibrations.

### B. Crystal Structure

The crystal structure of compound I (Fig. 1) is described in detail in Ref. [15] by Masmoudi *et al.*, where an isostructural analogue in which cobalt is replaced by copper is also reported. Here, we present a brief structural description that is relevant for the magnetic interpretation. Compound I crystallizes in the monoclinic system with space group $P2_1/c$ and features a dinuclear cobalt unit in which two equivalent Co ions are bridged by two $\mu$-adenine ligands and two $\mu$-$H_2O$ molecules. Each cobalt center is coordinated by two nitrogen atoms from the adenine ligands and four water molecules, completing a slightly distorted hexacoordinate environment. The structure exhibits a short Co–Co distance of 3.1241(6) Å (Fig. 2). Relevant bond distances for compound I are listed in Table II. Charge-balance considerations, together with four nitrate counter-ions, indicate a +2 oxidation state for both metal centers, corresponding to a $d^7$ electronic configuration. The crystallographic data and the refinement details are listed in I.

TABLE I. Crystal data and structure refinement for $[Co_2(\mu\text{-L1H})_2(\mu\text{-}H_2O)_2(H_2O)_4]4NO_3 \cdot 2H_2O$.

| **Compound** | 1 |
|---|---|
| Empirical formula | $C_{10}H_{26}Co_2N_{14}O_{20}$ |
| Formula weight | 780.31 |
| Crystal system | Monoclinic |
| Space group | $P2_1/c$ |
| $a$ (Å) | 10.3954(3) |
| $b$ (Å) | 18.9569(6) |
| $c$ (Å) | 7.3054(2) |
| $\alpha$ (°) | 90 |
| $\beta$ (°) | 103.6900(10) |
| $\gamma$ (°) | 90 |
| $V$ (Å$^3$) | 1398.74(7) |
| Temperature (K) | 150(2) |
| $Z$ | 2 |
| $\rho_{\mathrm{calc}}$ (g cm$^{-3}$) | 1.853 |
| $\mu$ (mm$^{-1}$) | 1.298 |
| $F(000)$ | 796 |
| Crystal size (mm$^3$) | $0.200 \times 0.040 \times 0.020$ |
| $2\theta$ range for data collection (°) | 2.285–29.178 |
| Index ranges | $-14 < h < 14$ |
| | $-25 < k < 25$ |
| | $-10 < l < 9$ |
| Reflections collected | 54,523 |
| Independent reflections | 3723 [$R_{\mathrm{int}} = 0.0357$] |
| Final $R_1$, $wR_2$ [$I > 2\sigma(I)$] | 0.0305, 0.0700 |
| Final $R_1$, $wR_2$ (all data) | 0.0332, 0.0747 |
| Data/restraints/parameters | 3723/0/252 |
| Goodness-of-fit on $F^2$ | 1.133 |
| CCDC number | 2440,271 |

In an hexacoordinated ligand field, $Co^{II}$ can adopt either a high-spin state ($S = 3/2$) or, when surrounded by strong-field ligands, a low-spin state ($S = 1/2$). The weak-field character of the bridging and terminal water molecules present here stabilises the high-spin $^4T_{1g}$ ground term.[13, 14, 18] Strong spin–orbit coupling within this term generates pronounced magnetic anisotropy, reflected in sizeable zero-field-splitting parameters $D$ and $E$ [19–21].

TABLE II. Selected bond lengths (Å) for compound I $[Co_2(\mu\text{-L1H})_2(\mu\text{-}H_2O)_2(H_2O)_4]4NO_3 \cdot 2H_2O$; (i = symmetry operation [-x+2,-y+1,-z+1])

| Bond | Distance (Å) |
|---|---|
| Co(1)–O(1) | 2.1614(12) |
| Co(1)–O(2) | 2.0439(13) |
| Co(1)–O(3) | 2.0445(14) |
| Co(1)–N(9i) | 2.1199(13) |
| Co(1)–N(3) | 2.1435(14) |
| Co(1)–O(1i) | 2.1780(12) |

Axial distortions further split the $t_{2g}$ manifold, while relativistic effects modulate its separation from the $e_g$ set. Together, these factors govern the effective spin–orbit coupling and, consequently, the temperature-dependent magnetic susceptibility and hysteresis observed for $Co^{II}$

complexes [20, 22, 23].

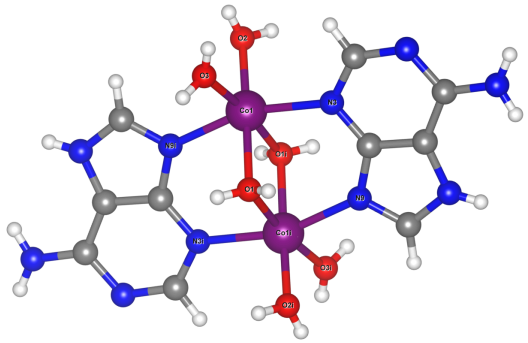

FIG. 1. Molecular structure of compound 1; (i = symmetry operation [-x+2,-y+1,-z+1]). Nitrate counter-ions and water molecules were omitted for clarity.

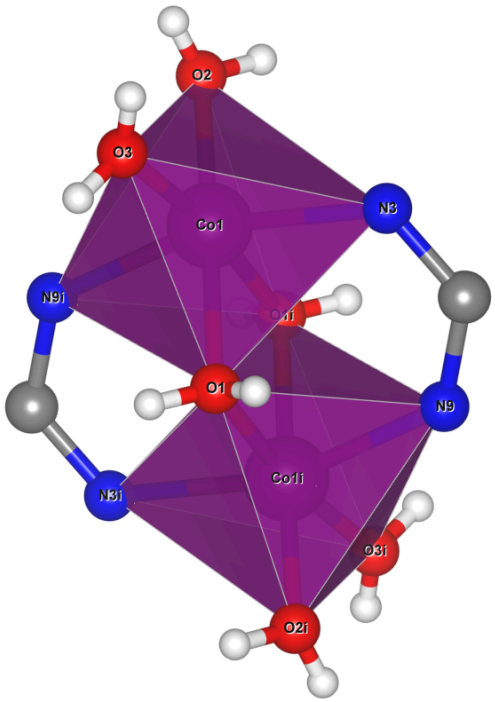


FIG. 2. Polyhedral representation of compound I; (i = symmetry operation [-x+2,-y+1,-z+1]). Nitrate counter-ions, water molecules, and aromatic rings have been omitted for clarity.

### C. Magnetic data

Magnetic measurements were conducted using a PPMS platform (Physical Property Measurement System) following the guidelines of Quantum Design systems. The magnetic properties of compound I were investigated in a polycrystalline sample through isothermal magnetization curves in the magnetic field range from 0 T to 9 T, and isofield magnetization in the temperature range of 2 K to 300 K. As the material does not exhibit long-range magnetic order, no special treatment was needed. The isofield magnetization data were subsequently used to calculate the magnetic susceptibility according to $\chi(T) = M(T)/B$, where $M(T)$ is the magnetization and $B$ is the constant applied magnetic field. To quantitatively analyze the magnetic properties, the experimental $\chi T$ data were fitted using the DAVE-MagProp software [24]. In this approach, the magnetic susceptibility is calculated as the orientational average, $\chi = (\chi_x + \chi_y + \chi_z)/3$, and the goodness of the fit is assessed using Pearson's chi-squared criterion. The quality of the fit was evaluated through the reduced chi-squared value, yielding $\chi^2_{\text{red}} = 0.09$, which indicates an excellent agreement between the experimental data and the model, as shown in the left panel of Fig. 4. The same set of parameters obtained from the fit of $\chi T$ was subsequently used to fit the field-dependent magnetization, as shown in the right panel of Fig. 4. As can be seen, the excellent agreement between the susceptibility and magnetization fits using this parameter set strongly validates the robustness of the applied magnetic model.

At 3 K, the magnetization approaches saturation at $B = 9$ T, reaching a value of $\mathrm{M}^{\text{exp}} = 4.33\ N_A\mu_B$, which is significantly lower than the theoretical saturation limit $\mathrm{M}^{\text{theo}} = g_{\text{iso}}S_{\text{max}} = 6\ N_A\mu_B$, assuming $g_{\text{iso}} = 2$ and $S_{\text{max}} = 3$. This reduced saturation magnetization indicates the presence of magnetic anisotropy, in addition to an antiferromagnetic exchange interaction between the two Co atoms.

A similar effect is observed in the $\chi T$ versus temperature curve shown in left panel of Fig. 4. At high temperatures, the magnetic susceptibility follows the Curie law, for which $\chi T = C$ remains constant, where $C = 2g^2\mu_B^2 S_{max}(S_{max}+1)/3k_B$. The theoretical Curie constant per dimer is $C^{\text{theo}} = 6.72\mu_B \cdot \text{K/FU} \cdot T$, whereas the experimental value extracted from the $\chi T$ data is significantly larger, $C^{\text{exp}} = 10.61\mu_B \cdot \text{K/FU} \cdot T$, exceeding the spin-only prediction. This substantial enhancement can be attributed to strong spin–orbit coupling effects, which increase the effective Landé factor, as well as the presence of zero-field splitting. For these reasons, in the following analysis we will assume that both Co ions remain in the HS state and explicitly include the ZFS anisotropy term in the effective Hamiltonian introduced in the next section.

## III. EFFECTIVE HAMILTONIAN

The crystal structure of the system leads to the inclusion of a Heisenberg exchange interaction term. To account for the anisotropic effects arising from the partial quenching of the orbital angular momentum and the coordination environment of Co(II), the model incorporates axial ($D$) and rhombic ($E$) anisotropy parameters. As both Co(II) ions are symmetric and exhibit the same hexacoordination, the axial and rhombic pa-

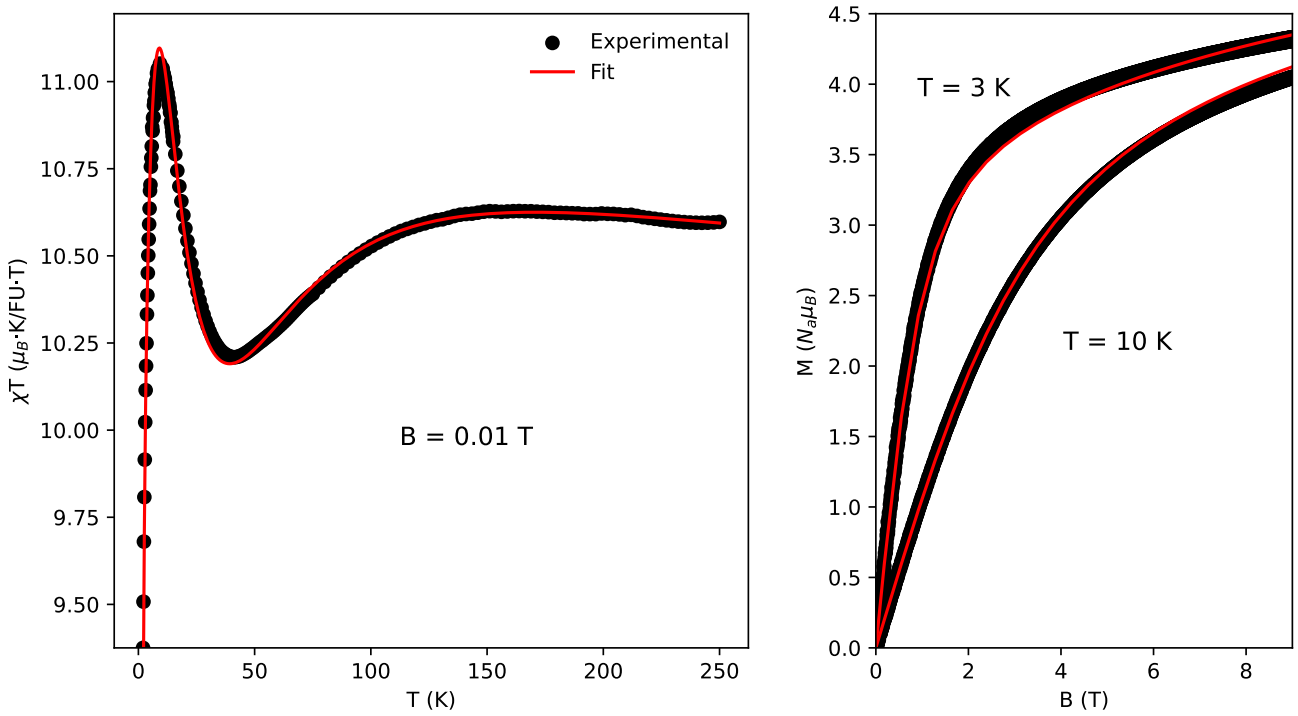


FIG. 3. Experimental data (circles) and theoretical fit (solid red line) of $\chi T$ (left panel) and field dependence of the magnetization (right panel) for $[Co_2(\mu\text{-L1H})_2(\mu\text{-}H_2O)_2(H_2O)_4]4NO_3 \cdot 2H_2O$. The strong agreement between the susceptibility and magnetization fits using this parameter set underscores the robustness and reliability of the extracted parameters.

rameters are identical for both atoms. These anisotropy parameters significantly influence the magnetic properties of Co(II) complexes, as they are governed by the crystal field and spin–orbit coupling. Notably, previous studies have demonstrated that pronounced anisotropy in hexacoordinated Co(II) complexes results from the interplay between spin–orbit coupling and distortions in the coordination geometry [18]. Inter-dimer couplings were neglected, since the distance between Co dimers is 7.3 Å. Furthermore, no experimental evidence of long-range magnetic ordering was observed, supporting this assumption. Consequently, we propose the effective Hamiltonian given by:

$$\mathcal{H} = -J\vec{S}_1 \cdot \vec{S}_2 + \sum_{i=1}^{2} \left\{ D\left(S_{iz}^2 - \frac{1}{3}S_i^2\right) + E\left(S_{ix}^2 - S_{iy}^2\right) - \mu_B \vec{B} \cdot \overleftrightarrow{g} \cdot \vec{S}_i \right\} \quad (1)$$

where $S_i$ $(i = 1, 2)$ represents the spin operators for both Co(II) in the high-spin state, $\overleftrightarrow{g}$ is the diagonal tensor for the Landé factors $g_x$, $g_y$ and $g_z$. These Landé factors are crucial in understanding the magnetic anisotropy of Co(II) complexes, as highlighted in [21]. Spectroscopic investigations have demonstrated that the variation of the gyromagnetic ratio $g$ along different crystallographic axes can provide valuable insights into electronic distribution and ligand interactions, as discussed in reference [23]. Additionally, EPR studies have shown that refined gyromagnetic ratios can be used to establish correlations between magnetic anisotropy and zero-field splitting parameters, as reported in [22].

TABLE III. Fitted parameters obtained from the magnetic susceptibility-temperature ($\chi T$) data for compound I.

| Compound | $J$ (K) | $D$ (K) | $E$ (K) | $g_x$ | $g_y$ | $g_z$ |
|---|---|---|---|---|---|---|
| **I** | -8.6(8) | 89(5) | 23(2) | 2.5(1) | 2.5(1) | 2.4(1) |

This effective Hamiltonian was used to calculate the average powder $\chi$T as a function of temperature, with the model parameters optimized to fit the experimental data (see the left panel of Fig. 4). Additionally, diamagnetic contributions ($\chi_D = -1.8 \cdot 10^{-4}\ \mu_B/\text{FU} \cdot T$) from the

TABLE IV. Magnetic exchange and anisotropy parameters for several hexacoordinated dinuclear Co(II) complexes.

| Compound | $J$ (K) | $D$ (K) | $g_x$ | $g_y$ | $g_z$ |
|---|---|---|---|---|---|
| $[Co_2(\mu\text{-L1H})_2(\mu\text{-}H_2O)_2(H_2O)_4]4NO_3 \cdot 2H_2O$ | -8.6 | 89 | 2.5 | 2.5 | 2.4 |
| $[Co_2(3\text{-fuc})_4(\text{isonia})_4]^a$ | -2.53 | 90.21 | 2.527 | 2.527 | 2 |
| $[Co_2(2\text{-fuc})_4(\text{isonia})_4]^a$ | -3.44 | 52.34 | 2.5 | 2.5 | 2 |
| $[Co_2(H_2O)(PhCO_2)_4(py)_4] \cdot 0.5(PhCO_2H) \cdot 1.5(MePh)^b$ | -1.57 | 132.9 | 2.52 | 2.52 | 2.17 |
| $[Co_2(H_2O)(PhCO_2)_4(Mepy)_4]^b$ | -1.01 | 72.9 | 2.31 | 2.31 | 2.01 |
| $[Co_2(H_2O)(PhCO_2)_4(iqu)_4] \cdot iqu^b$ | -3.49 | 143.3 | 2.54 | 2.54 | 2.00 |
| $[Co_2(H_2O)(PhCO_2)_4(fupy)_4]^b$ | -1.29 | 98.8 | 2.54 | 2.54 | 2.00 |
| $[Co_2(H_2O)(PhCO_2)_4(Mefupy)_4]^b$ | -2.34 | 114.9 | 2.70 | 2.70 | 2.59 |
| $[Co_2(H_2O)(PhCO_2)_4(Me_2fupy)_4]^b$ | -1.61 | 111.5 | 2.74 | 2.74 | 2.54 |

Note: Superscripts $^a$ and $^b$ refer to values taken from Refs. [25] and [26], respectively. It is worth noting that the analysis in Ref. $^a$ does not include the rhombic anisotropy parameter $E$. In contrast, Ref. $^b$ adopts a more general description of the magnetic behavior, incorporating non-diagonal components of the $D$-tensor, which also does not include the rhombic term.

system were also included. The same model was also employed to fit the magnetization as a function of the applied magnetic field, as shown in the right panel of Fig. 4. The resulting fitted parameters are listed in Table III.

## IV. RESULTS AND DISCUSSION

At first glance, the exchange constant $J = -8.6$ K indicates antiferromagnetic coupling between the cobalt ions, consistent with the reduction of $\chi T$ as the temperature approaches the exchange energy scale. This trend is clearly observed in the left panel of Fig.4, where $\chi T$ decreases as $T \to 0$, reflecting the stabilization of a singlet ground state and the consequent suppression of the magnetic susceptibility. Hexacoordinated high-spin Co(II) dimers can exhibit either antiferromagnetic or ferromagnetic coupling behavior depending on how the bridging occurs between the metal centers, as the magnetic interaction is usually governed by superexchange pathways. Numerous examples can be found in the literature, for instance, both $[Co_2(\mu\text{-OAc})_2(\mu\text{-AA})(\text{urea})(\text{tmen})_2][OTf]$ and $[Co_2(\mu\text{-}H_2O)(\mu\text{-OAc})_2(OAc)_2(\text{tmen})_2]$ exhibit antiferromagnetic coupling, with J = -5.18 K and J = -1.01 K, respectively, whereas $[Co_2(\mu\text{-OAc})_3(\text{urea})(\text{tmen})_2][OTf]$ shows ferromagnetic coupling with J = 25.89 K [27] due to the substitution of the hydroxamate.

Furthermore, the obtained axial and rhombic zero-field splitting parameters are $D = 89$ K and $E = 23$ K, respectively, which are characteristic of systems where the electronic states experience significant crystal field splitting. This magnetic anisotropy is also reflected in the Landé factors, with fitted values $g_x = g_y = 2.5$ and $g_z = 2.4$, indicating that the $xy$ plane is the easy plane of magnetization, consistent with the positive value of D and the condition $g_x, g_y > g_z$. Although different effective Hamiltonians are commonly employed in the literature, this anisotropic behavior is frequently observed in Co(II) dimers, where D is typically positive and $g_x, g_y > g_z$, for instance, the six dinuclear Co(II) complexes [25] modeled by a general bilinear exchange shows large values of D ranging from 71.9 K to 143.8 K, where all the complexes are antiferromagnetic with a easy plane magnetization. Representative examples include $[Co_2(3\text{-fuc})_4(\text{isonia})_4]$ and $[Co_2(2\text{-fuc})_4(\text{isonia})_4]$ [26], which were modeled using a similar Hamiltonian without the rhombic term. For these compounds, the reported parameters are $g_x = g_y = 2.527$, $g_z = 2$, and $D = 90.21$ $K$ for the first complex, and $g_x = g_y = 2.5$, $g_z = 2$, and $D = 52.34$ $K$ for the second one, which also shows a easy plane behavior and antiferromagnetic coupling. The parameters of these complexes can be seen in Table IV.

## V. CONCLUSIONS

In summary, the present study offers a quantitative magnetic characterization of a hexacoordinated cobalt(II) dimer, with emphasis on its anisotropy

and exchange coupling, as determined from a consistent analysis of susceptibility and magnetization data. The dinuclear Co(II) molecular magnet $[Co_2(\mu\text{-}L1H)_2(\mu\text{-}H_2O)_2(H_2O)_4] \cdot 4NO_3 \cdot 2H_2O$, that have been structurally characterized, were successfully subjected to the magnetochemical analysis, where both hexacoordinated Co(II) centers are antiferromagnetically coupled ($J = -8.6\ K$) and exhibit pronounced axial ($D = 89\ K$) and rhombic anisotropy ($E = 23\ K$), consistent with previous studied metal complexes in the literature. This anisotropy were also captured in the parameters the anisotropic Landé factors, where $g_x = g_y = 2.5$ and $g_z = 2.4$, showing a easy plane magnetization for which can be further corroborated by high-frequency EPR. In addition, it is worth highlighting that the consistency between the fits of the susceptibility and magnetization data with the set of parameters obtained supports the reliability of the applied magnetic model. Therefore, by presenting a new example of a dinuclear Co(II) complex with comprehensively characterized magnetic anisotropy, this work furnishes additional experimental data that advances the fundamental understanding of spin–orbit coupling phenomena in molecular magnetic systems.

## ACKNOWLEDGMENTS

CC thanks the Fundação de Amparo à Pesquisa do Estado da Bahia - FAPESB for its financial support (grant numbers APP0041/2023 and PPP0006/2024). This research received partial funding from the Coordenação de Aperfeiçoamento de Pessoal de Nível Superior – Brasil (CAPES) under Finance Code 001. MSR expresses gratitude to FAPERJ and CNPq, while AS is thankful to CAPES for their financial support (grant number 88887.001022/2024-00). LG thanks the Fundação de Amparo à Pesquisa do Estado do Rio de Janeiro - FAPERJ for its financial support (grant number E-26/211.270/2021). This study was financed, in part, by the São Paulo Research Foundation (FAPESP), Brasil. Process Number 2025/21289-6.

## REFERENCES

[1] M. S. Reis. Magnetocaloric and barocaloric effects of metal complexes for solid state cooling: Review, trends and perspectives. *Coord. Chem. Rev.*, 523:43, 2012.

[2] F. S. Guo, B. M. Day, Y. C. Chen, M. L. Tong, A. Mansikkamäki, and R. A. Layfield. Magnetic hysteresis up to 80 kelvin in a dysprosium metallocene single-molecule magnet. *Science*, 362(6421):1400–1403, 2018. Epub 2018 Oct 18.

[3] L. Bogani and W. Wernsdorfer. Molecular spintronics using single-molecule magnets. *Nat. Mater.*, 7:179, 2008.

[4] R. Sen, S. D. P. De, A. M. dos Santos, L. B. L. Escobar, P. C. Brandão, F. A. A. Paz, M. S. Reis, and Z. Lin. Novel $co_5$ cluster based triazole bridged cobalt-fluorophosphate: Synthesis, structure, magnetic and heterogeneous catalytic epoxidation studies. *European Journal of Inorganic Chemistry*, 2023(26):e202300174, 2023.

[5] R. Sen, K. Mondal, A. M. dos Santos, L. B. L. Escobar, P. Brandão, M. S. Reis, and Z. Lin. A chiral alkali metal capped $ni_4$ cubane complex: Synthesis, structure, magnetic and catalytic bromination studies. *Journal of Molecular Structure*, 1274, 2023.

[6] B. J. M. L. Ferreira, P. Brandão, M. Meireles, F. Martel, A. Correia-Branco, D. M. Fernandes, T. M. Santos, and V. Félix. Synthesis, structural characterization, cytotoxic properties and dna binding of a dinuclear copper(ii) complex. *Journal of Inorganic Biochemistry*, 161:9–17, 2016.

[7] B. Ari, M. Das, P. Brandao, S. Mukherjee, A. D. Jana, B. Koley, S. Laha, M. M. Islam, I. Choudhuri, N. Bhattacharya, B. C. Samanta, N. Chattopadhyay, and T. Maity. Dna/hsa binding and anticancer properties of pendant acetate bearing mono-nuclear ni(ii) and bridging acetate bearing di-nuclear cu(ii) schiff base complexes: an experimental and molecular docking study. *New Journal of Chemistry*, 47(38):17881–17896, 2023.

[8] L. Habala, L. Pašková, A. Bilková, F. Bilka, B. Oboňová, and J. Valentová. Antimicrobial activity and cytotoxicity of transition metal carboxylates derived from agaric acid. *European Pharmaceutical Journal*, 68(1):46–53, January 2021.

[9] Ganesan Kumaravel, Ponnukalai Ponya Utthra, and Natarajan Raman. Dna fastening and scission actions of cu(ii), co(ii), ni(ii) and zn(ii) complexes: synthesis, spectral characterization and cytotoxic study. *Applied Organometallic Chemistry*, 32(2), September 2017.

[10] Hasene Mutlu Gençkal, Merve Erkisa, Pınar Alper, Saliha Sahin, Engin Ulukaya, and Ferda Ari. Mixed ligand complexes of co(ii), ni(ii) and cu(ii) with quercetin and diimine ligands: synthesis, characterization, anti-cancer and anti-oxidant activity. *JBIC Journal of Biological Inorganic Chemistry*, 25(1):161–177, December 2019.

[11] Clebson Cruz, Maron F Anka, Mario S Reis, Romain Bachelard, and Alan C Santos. Quantum battery based on quantum discord at room temperature. *Quantum Science and Technology*, 7(2):025020, mar 2022.

[12] Clebson Cruz, Hamid-Reza Rastegar-Sedehi, Maron F Anka, Thiago R de Oliveira, and Mario Reis. Quantum stirling engine based on dinuclear metal complexes. *Quantum Science and Technology*, 8(3):035010, may 2023.

[13] Mario Reis. *Fundamentals of magnetism*. Elsevier, 2013.

[14] Olivier Kahn. *Molecular magnetism*. Courier Dover Publications, 2021.

[15] Mariem Masmoudi, Cláudia Silva, Nelson Andrade, Fátima Martel, and Paula Brandão. Coordination complexes of co, cu, and fe with adenine and phenanthroline: Synthesis, characterization, and cytotoxic studies. *Journal of Molecular Structure*, 1345:143128, 2025.

[16] C. Cruz, D. O. Soares-Pinto, P. Brandão, A. M. dos Santos, and M. S. Reis. Carboxylate-based molecular magnet: One path toward achieving stable quantum correlations at room temperature. *EPL (Europhysics Letters)*, 113(4):40004, February 2016.

[17] A. M. Souza, D. O. Soares-Pinto, R. S. Sarthour, I. S. Oliveira, M. S. Reis, P. Brandão, and A. M. dos Santos. Entanglement and bell's inequality violation above room temperature in metal carboxylates. *Physical Review B*, 79(5), February 2009.

[18] S.M Ostrovsky, R Werner, David A Brown, and

W Haase. Magnetic properties of dinuclear cobalt complexes. *Chemical Physics Letters*, 353(3):290–294, 2002.

[19] Arun Kumar Bar, Céline Pichon, and Jean-Pascal Sutter. Magnetic anisotropy in two- to eight-coordinated transition–metal complexes: Recent developments in molecular magnetism. *Coordination Chemistry Reviews*, 308:346–380, 2016. Perspectives in Coordination Chemistry on the Occasion of the 40th anniversary of the LCC-CNRS, Toulouse, France.

[20] Radovan Herchel, Lucia Váhovská, Ivan Potočňák, and Zdeněk Trávníček. Slow magnetic relaxation in octahedral cobalt(ii) field-induced single-ion magnet with positive axial and large rhombic anisotropy. *Inorganic Chemistry*, 53(12):5896–5898, 2014. PMID: 24853769.

[21] Alexander A. Pavlov, Joscha Nehrkorn, Sergey V. Zubkevich, Matvey V. Fedin, Karsten Holldack, Alexander Schnegg, and Valentin V. Novikov. A synergy and struggle of epr, magnetometry and nmr: A case study of magnetic interaction parameters in a six-coordinate cobalt(ii) complex. *Inorganic Chemistry*, 59(15):10746–10755, 2020. PMID: 32672944.

[22] Subrata Ghosh, Sujit Kamilya, Mayurika Das, Sakshi Mehta, Marie-Emmanuelle Boulon, Ivan Nemec, Mathieu Rouzières, Radovan Herchel, and Abhishake Mondal. Effect of coordination geometry on magnetic properties in a series of cobalt(ii) complexes and structural transformation in mother liquor. *Inorganic Chemistry*, 59(10):7067–7081, 2020. PMID: 32378897.

[23] Alexander A. Pavlov, Svetlana A. Savkina, Alexander S. Belov, Yulia V. Nelyubina, Nikolay N. Efimov, Yan Z. Voloshin, and Valentin V. Novikov. Trigonal prismatic tris-pyridineoximate transition metal complexes: A cobalt(ii) compound with high magnetic anisotropy. *Inorganic Chemistry*, 56(12):6943–6951, 2017. PMID: 28541691.

[24] R. T. Azuah, L. R. Kneller, Y. Qiu, P. L. Tregenna-Piggott, C. M. Brown, J. R. Copley, and R. M. Dimeo. Dave: A comprehensive software suite for the reduction, visualization, and analysis of low energy neutron spectroscopic data. *Journal of Research of the National Institute of Standards and Technology*, 114(6):341–358, 2009.

[25] J Hudák, R Boča, J Moncol, and J Titiš. Magnetism of dinuclear benzoato cobalt(II) complexes modeled by a general bilinear exchange. *Inorganica Chim. Acta*, 394:401–409, January 2013.

[26] Jakub Mihalčiak, Petra Bertová, Zdeňka Růžičková, Ján Moncol, Peter Segľa, and Roman Boča. Structure and magnetism of novel dinuclear cobalt(II) complexes. *Inorg. Chem. Commun.*, 56:62–64, June 2015.

[27] S. Ostrovsky, Z. Tomkowicz, and W. Haase. High-spin co(ii) in monomeric and exchange coupled oligomeric structures: Magnetic and magnetic circular dichroism investigations. *Coordination Chemistry Reviews*, 253(19):2363–2375, 2009.

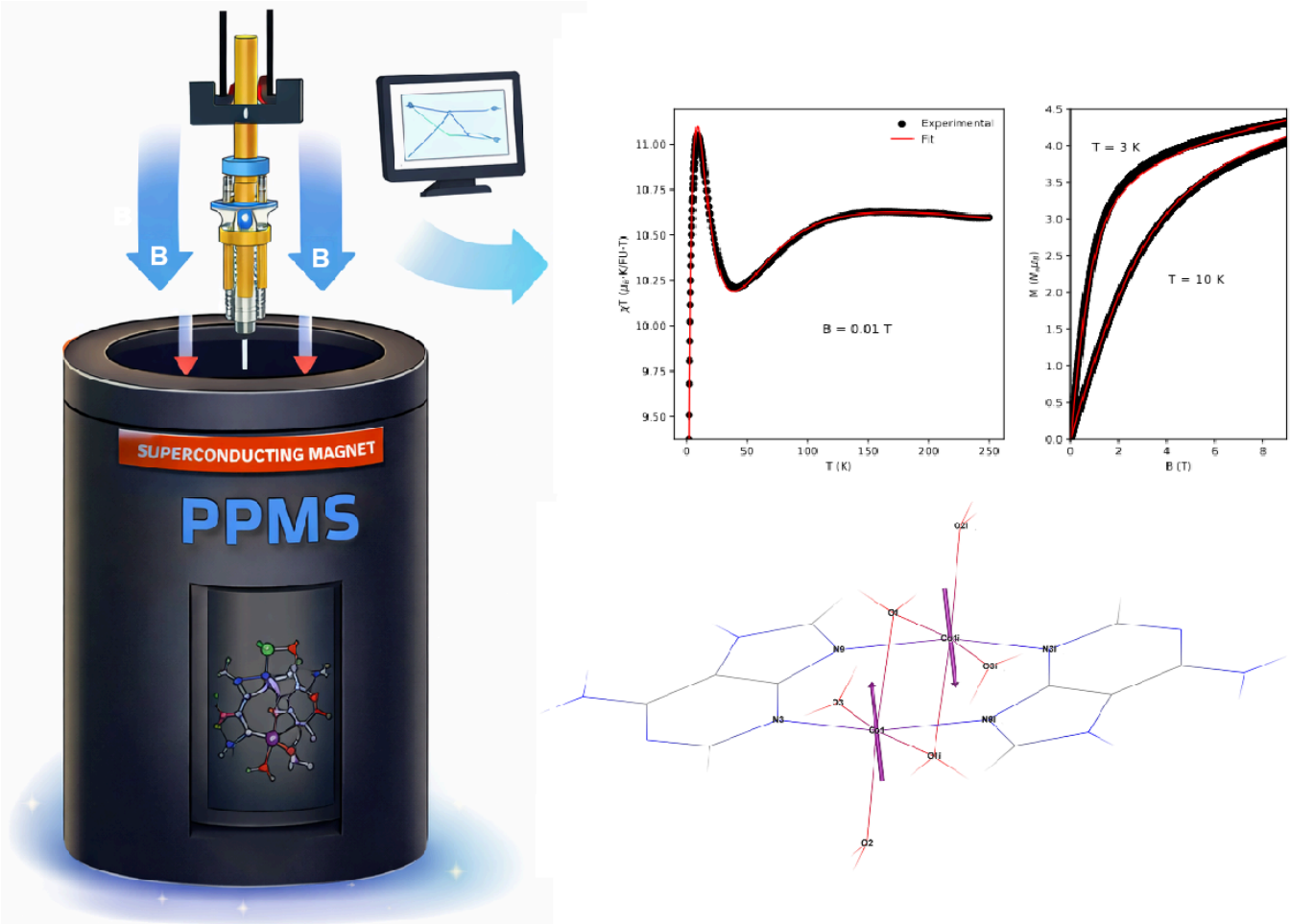


FIG. 4. TOC Graphic